Research Paper

PAIN®

Altered brain structure and function associated with sensory and affective components of classic trigeminal neuralgia

Yuan Wang[a,b,c], Dong-yuan Cao[b,c], Bethany Remeniuk[d,e], Samuel Krimmel[c,d], David A. Seminowicz[c,d], Ming Zhang[a,*]

Abstract

Classic trigeminal neuralgia (CTN) is a chronic neuropathic pain state characterized by intense, piercing spasms of the orofacial region, and may be attributable to abnormal pain processing in the central nervous system. Our study investigated neuronal alterations using voxel-based morphometry (VBM), diffuse tensor imaging (DTI), and resting-state functional connectivity in 38 patients with CTN and 38 matched healthy controls. For voxel-based morphometry analyses, patients with CTN displayed gray matter volume (GMV) reductions in the anterior-cingulate cortex (ACC) and mid-cingulate cortex, insula, secondary somatosensory cortex (S2), primary motor cortex (M1), premotor area, and several regions in the temporal lobe. For DTI analysis, patients compared with controls had increased mean diffusivity (MD) and decreased fractional anisotropy (FA) in the corpus callosum and the bilateral corona radiata, and increased mean diffusivity with no fractional anisotropy changes across the bilateral superior longitudinal fasciculus, the internal and external capsule, the thalamus and brainstem. Additionally, patients with CTN had enhanced functional connectivity between the right insula/S2 and ACC, medial prefrontal cortex, posterior cingulate cortex, and bilateral dorsolateral prefrontal cortex. Furthermore, gray matter volume of left inferior temporal gyrus negatively correlated with current pain intensity and disease duration in patients, and connectivity of the right insula/S2-ACC was negatively correlated with pain intensity, depression, and anxiety ratings. This study provides multiple lines of evidence supporting aberrant structural and functional patterns that are observed in patients with CTN, which may help us better understand the pathophysiology of CTN and facilitate the development of new therapies for this disease.

Keywords: Trigeminal neuropathic pain, Voxel-based morphometry, Diffusion tensor imaging, Tract-based spatial statistics, Resting-state functional connectivity

1. Introduction

Classic trigeminal neuralgia (CTN) is a severe paroxysmal pain disorder characterized by unilateral lancinating attacks in one or more of the trigeminal nerve branches. These attacks can be triggered by innocuous tactile stimuli or occur spontaneously. Unlike other neuropathic pain conditions, patients with CTN are often pain-free between attacks. However, coinciding with disease progression, attacks subsequently become more frequent and sustained.[6]

The etiology of CTN remains unclear, but some studies suggest that CTN is due to microvascular compression of the trigeminal root by aberrantly formed blood vessels, called nerve vessel conflict (NVC).[1,30] These loops may lead to demyelination and axonopathy, increasing hyperexcitability of the trigeminal root and ganglion, which may induce pain paroxysms.[14] However, NVC is not exclusive to patients with CTN, as an estimated 49% of the healthy population exhibit contact without deviation or mild deviation of the nerves by the vasculatures.[22] Moreover, despite upward of 75% of patients with CTN receive pain relief after neurosurgical intervention named microvascular decompression, approximately 30% of the patients experience recurrence of the facial pain.[62] It has been proposed that NVC may represent a risk factor for the development of CTN but not a single etiologic factor. The peripheral mechanisms alone do not sufficiently explain CTN, and involvement of central nervous system[15] and the interaction between central and peripheral mechanisms[17] better account for the symptoms. Therefore, it is necessary to investigate the morphometric brain alterations in patients with CTN.

Because relatively little is known about the initiation and maintenance of CTN, it is important to elucidate the underlying neuronal differences between those with CTN and healthy population at large. Neuroimaging studies have demonstrated that chronic pain is associated with morphometric brain changes as well as altered functional connectivity, eg, altered

Sponsorships or competing interests that may be relevant to content are disclosed at the end of this article.

[a] *Department of Medical Imaging, First Affiliated Hospital of Xi'an Jiaotong University, Xi'an, P.R. China,* [b] *Key Laboratory of Shaanxi Province for Craniofacial Precision Medicine Research, Stomatological Hospital, Xi'an Jiaotong University, Xi'an, P.R. China,* [c] *Department of Neural and Pain Sciences, School of Dentistry, University of Maryland Baltimore, Baltimore, MD, USA,* [d] *Center to Advance Chronic Pain Research, University of Maryland Baltimore, Baltimore, MD, USA,* [e] *Department of Psychiatry and Behavioral Sciences, Johns Hopkins University School of Medicine, Baltimore, MD, USA*

**Corresponding author. Address: Department of Medical Imaging, First Affiliated Hospital of Xi'an Jiaotong University, 277 West Yanta Rd, Xi'an, Shaanxi, P.R. China 710061. Tel.: +86-18991232265; fax: +86-2985323428. E-mail address: profzmmri@126.com (M. Zhang).*

PAIN 158 (2017) 1561–1570

http://dx.doi.org/10.1097/j.pain.0000000000000951

default mode network (DMN) connectivity.[4,11,12,23] In CTN, voxel-based morphometry (VBM) studies have reported gray matter changes in the anterior and posterior insula, anterior cingulate cortex (ACC), primary/secondary somatosensory cortex (S1/S2), dorsolateral prefrontal cortex (DLPFC), and thalamus,[18,20,39] in addition to extensive white matter alterations.[34,61] One task-related functional magnetic resonance imaging (MRI) study suggested a state of maintained sensitization of the trigeminal nociceptive systems in CTN[35] but there is limited data on disruptions of resting-state connectivity in patients with CTN.

Some links have been reported between CTN and psychiatric disorders. For example, a retrospective investigation suggested that patients with trigeminal neuralgia are approximately 2.85 and 2.98 times more likely to suffer from depressive and anxiety disorders than matched controls,[58] and another study demonstrated a substantial patient burden expressed as interference with daily functioning and reduced health status associated with severity of CTN.[49] But the relationship between indices of structural and functional MRI in the brain and emotional alterations in patients with CTN still remains unclear.

The aim of this study was to investigate the alterations of VBM, diffuse tensor imaging, and functional connectivity in patients with CTN, and explore the correlations between structural and functional deficits and clinical variables. We hypothesized that patients with CTN have potentially abnormal gray matter volume (GMV) and/or white matter diffusivity, and the intermittent, lancinating pain may link to the alterations in functional connectivity in brain regions associated with nociception.

2. Materials and methods

2.1. Participants

Forty-one patients with CTN and 40 age- and sex-matched healthy controls were recruited prospectively from the First Affiliated Hospital of Xi'an Jiaotong University. All participants were right-handed according to self-report. The diagnosis of CTN was confirmed by 2 neurologists according to the International Classification of Headache Disorders (ICDH-III).[46] Inclusion criteria included: disease duration >2 years; unilateral pain in the distribution of one or more branches of the trigeminal nerve; intense and stabbing painful paroxysms from trigger areas or by trigger factors; and no neurological deficit or sensory loss. Exclusion criteria included: symptomatic or atypical neuralgia; previous microvascular decompression surgery or other invasive treatments for CTN; presence of any other pain disorders; or major psychiatric disorders. Most of the patients took carbamazepine for pain treatment and a small portion used oxcarbazepine and phenytoin, others took neurotrophic drugs such as mecobalamine and oryzanol. Consent was obtained according to the Declaration of Helsinki, and all research procedures were performed with permission of the ethics committee of the First Affiliated Hospital of Xi'an Jiaotong University.

2.2. Questionnaires and ratings

All participants were asked to rate the extent of their neuralgia-induced pain intensity using a visual analogue scale (VAS) under the supervision of a technician. The VAS was graded on a scale of 0 to 10 for the last 7 days, and the mean was then calculated.[56] Participants also completed the evaluations of anxious and depressive symptoms using the Hamilton Depression Rating Scale (HAMD) and the Hamilton Anxiety Rating Scale (HAMA),[55] which were reviewed by a psychiatrist. The technician and the psychiatrist were blinded to the experimental groups.

2.3. Magnetic resonance imaging data acquisition

Imaging data were collected on a 3.0-T scanner (Signa HDxt; GE Medical Systems, Waukesha, WI, USA), equipped with an 8-channel phased-array head coil. For each subject, a high-resolution structural image was acquired using axial fast spoiled gradient recalled sequence (field of view: 256 × 256 mm; matrix: 256 × 256; time of repetition = 2300 ms; time of echo = 4.9 ms; resolution = 1.00 × 1.00 mm; flip angle: 15.0°). The resting-state functional magnetic resonance imaging (rsfMRI) data were obtained using echo planar imaging (150 volumes; 35 contiguous slices/volume; FOV: 240 × 240 mm; matrix: 64 × 64; spatial resolution = 3.75 × 3.75 × 4 mm; TR = 2000 ms; TE = 35 ms; flip angle: 90°). During the rsfMRI, subjects were instructed to stay awake but to keep their eyes closed. A diffusion tensor image (DTI) scan was also conducted (35 contiguous slices; FOV: 240 × 240 mm; matrix: 128 × 128; spatial resolution = 1.88 × 1.88 × 4 mm; direction: 30; = 10,000 ms; TE = 87.3 ms).

2.4. Magnetic resonance imaging data preprocessing and analysis

2.4.1. Voxel-based morphometry

Voxel-based morphometry analysis was performed using the DPARSF toolbox (State Key Laboratory of Cognitive Neuroscience and Learning, Beijing Normal University, Beijing, China) with Statistical Parametrical Mapping 8 (SPM8; http://www.fil.ion.ucl.ac.uk/spm) in MATLAB (Mathworks, Inc, Natick, MA). Voxel-wise GMV was analyzed between patients with CTN and control subjects. Anatomical images were firstly segmented into gray matter, white matter, and cerebrospinal fluid (CSF), spatially normalized with diffeomorphic anatomical registration through exponentiated Lie algebra (DARTEL) to the subject-specific template, and then smoothed with an isotropic Gaussian kernel of 8 mm full width at half maximum. Total intracranial volume, total GMV, white matter volume , and CSF were calculated and averaged for each group. Group difference on voxel-wise GMV images with total GMV, age, and sex as covariants were performed with a cluster forming (voxel-wise) threshold of uncorrected $P = 0.001$ and then corrected for multiple comparisons at the cluster level ($P = 0.05$, false discovery rate correction).

2.4.2. Diffuse tensor imaging: whole brain tract–based spatial statistics

Diffuse tensor imaging data processing and analysis were carried out using FMRIB Software Library (FSL) software (http://www.fmrib.ox.ac.uk/fsl), which included eddycurrent correction, making a brain mask for the DTI data, "DTIFIT" to reconstruct diffusion tensors, and fractional anisotropy (FA) voxel-wise statistical measures using Tract-Based Spatial Statistics (TBSS). First, the effects of head movement and eddy currents were corrected in the raw DTI data, next BET v2.1 was used for brain mask extraction, and then FA images were generated by scaling the diffusion tensor to the DTI data using FMRIB's diffusion toolbox (FDT 3.0). Mean diffusivity (MD) images were calculated from the average of 3 eigenvalues of L1, L2, and L3. Tract-Based Spatial Statistics analyses

Table 1

Demographic and clinical characteristics of patients with CTN and healthy controls.

	Patients with CTN ($\bar{x}$ ± SD)	Healthy controls ($\bar{x}$ ± SD)	*P* (2-tailed)
Sex (female/male)	22/16	22/16	NA
Age, y	55.87 ± 8.38	55.89 ± 8.06	0.989
Duration of disease, y	7.05 ± 5.32	NA	NA
Attack frequency (times per day)	5.90 ± 5.83	NA	NA
Average duration of attack, min	1.32 ± 0.77	NA	NA
Score of VAS	5.79 ± 1.70	NA	NA
Score of HAMA	4.08 ± 3.37	0.36 ± 0.85	0.000*
Score of HAMD	4.24 ± 3.37	0.34 ± 0.85	0.000*
TIV (L)	1.403 ± 0.113	1.449 ± 0.102	0.074
GMV (L)	0.662 ± 0.048	0.687 ± 0.042	0.042†
WMV (L)	0.514 ± 0.054	0.529 ± 0.053	0.238
CSF (L)	0.228 ± 0.032	0.234 ± 0.027	0.276

P values are calculated based on independent-samples *t* test between 2 groups, as appropriate.
* $P < 0.001$.
† $P < 0.05$.
$\bar{x}$, mean value; CSF, cerebrospinal fluid; CTN, classic trigeminal neuralgia; GMV, gray matter volume; HAMA, Hamilton Anxiety Rating Scale; HAMD, Hamilton Depression Rating Scale; NA, not applicable; TIV, total intracranial volume; VAS, visual analogue scale; WMV, white matter volume.

were performed to examine differences in FA and MD between patients with CTN and healthy controls. In detail, all of the FA images were nonlinearly registered to a FMRIB58-FA standard space template (http://www.fmrib.ox.ac.uk/fsl/data/FMRIB58_FA.html) and aligned to the Montreal Neurological Institute space. The mean image of all aligned FA images was then created and thinned to provide a mean FA skeleton with the FA value threshold at 0.2.[44] Aligned FA data of all participants were projected onto this skeleton, and the resulting data were entered into voxel-wise statistics. A randomization procedure at 5000 times (FSL's randomise, Monte Carlo permutation test) was used to perform the group-wise statistics. Next, the MD images were also aligned into MNI space and projected onto the mean FA skeleton using the protocol of non-FA images in TBSS. The permutation-based nonparametric inferences within the framework of the general linear model were performed to investigate the differences between the patients and controls in FSL. The results were corrected using threshold-free cluster enhancement (TFCE) correction for multiple comparisons ($P = 0.05$, family-wise error rate corrected).

Group differences were further evaluated on skeletonized FA and MD in the white matter of the whole brain. To do this, we extracted mean FA and MD values across every voxel in the skeleton for each subject and performed a 2-tailed *t* test.

2.4.3. Resting-state functional magnetic resonance imaging connectivity

The rsfMRI data were preprocessed using the DPARSF toolbox and REST toolbox version 1.8 (www.restfmri.net).[47] The first 5 volumes were discarded to avoid transient signal changes before magnetization reached steady-state and subjects' adaptation to the fMRI scanning noise. Preprocessing steps included: slice timing correction; head motion correction; skull-stripping using BET; co-registration of the anatomical image to the mean functional image; segmentation of the anatomical gray matter, white matter and CSF; normalization to MNI152 standard template; smoothing with an 6-mm Gaussian kernel; and band-pass filtering at 0.01 to 0.1 Hz.[59]

Functional connectivity was performed using the seed-voxel correlation approach,[23] in which the time-course signal in a seed region is correlated with all voxels in the brain. Seeds were defined as 6-mm-radius spheres centered on the peak voxels for the GMV clusters showing significant differences between

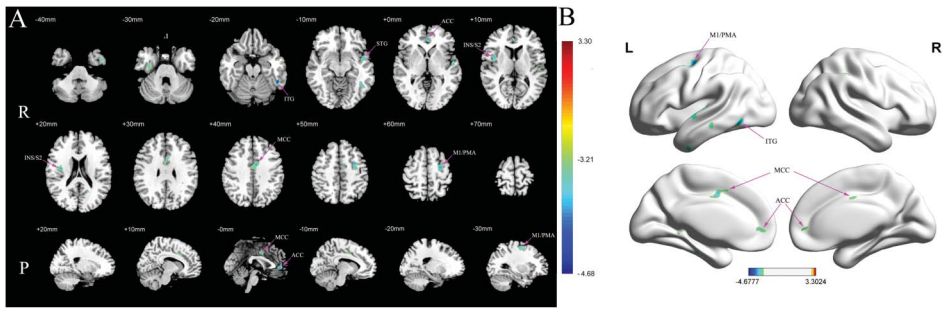

Figure 1. Regional gray matter volume decrease (blue–light blue) and increase (red–yellow) in patients with classic trigeminal neuralgia group in contrast to control subjects. (A) Axial, sagittal, and coronal views; (B) Lateral and medial views of bilateral hemispheres. All images were shown with FDR correction of $P = 0.05$ at a cluster level for multiple comparisons. The color bar displayed *t*-values. ACC, anterior cingulate cortex; INS, insula; ITG, inferior temporal gyrus; M1, primary motor cortex; MCC, middle cingulate cortex; PMA, premotor area; S2, secondary somatosensory cortex; STG, superior temporal gyrus.

Table 2

Peak MNI coordinates for regions exhibiting decreased GMV in the CTN group vs control group.

Anatomical regions	BA	Side	Voxels in cluster	MNI coordinate			Peak voxel *t* value	*P*
				x	y	z		
Controls > patients								
ACC	32	left	245	−1	38	1	3.8545	0.012
MCC	24	left	573	−6	−3	41	3.5209	0.029
ITG	20	left	391	−51	−48	−21	4.6777	0.006
ITG	20	right	188	53	−36	−27	3.2522	0.047
STG	41	left	340	−54	−14	4	3.4673	0.036
Insular cortex/S2	40/13	right	428	39	−1	15	3.7628	0.018
M1/PMA	4/6	left	512	−33	3	54	4.0361	0.009
Patients > controls								
SPL	7	right	72	28	−72	50	3.3024	0.042

Data are thresholded of $P = 0.05$ with FDR correction at the cluster level for multiple comparisons.
ACC, anterior cingulate cortex; BA, Brodmman area; CTN, classic trigeminal neuralgia; GMV, gray matter volume; ITG, inferior temporal gyrus; M1, primary motor cortex; MCC, middle cingulate cortex; PMA, premotor area; S2, secondary somatosensory cortex; SPL, superior parietal lobule; STG, superior temporal gyrus.

patients with CTN and controls. Two-sample *t* tests between the 2 groups were performed on each resultant connectivity map using total GMV as the covariance, with the cluster forming a threshold of $P = 0.005$ and then cluster-level corrected for multiple comparisons ($P = 0.05$, FDR correction).

2.4.4. Magnetic resonance imaging quality control

For VBM data, we inspected each volume for any artifact that could affect the processing, such as segmentation, normalization, etc. For DTI data, we looked at the constructed red-green-blue maps for each individual to ensure that all the major tracts were easily identified by eye. In addition, 4 subjects with head motion of any volume more than 1.5 mm or 1.5° were excluded in fMRI (2 patients and 2 controls) data preprocessing, and 1 CTN patient with prominent signal lose in the frontal lobe in raw DTI data was also ruled out from further analysis, leaving a total of 76 participants (38 patients and 38 controls) in the study.

2.5. Correlations with clinical variables

SPSS software version 18.0 (IBM Corporation, Armonk, NY) was used for the correlation analyses. To test whether the results from group comparisons for GMV, DTI, and rsfMRI for patients with CTN were related to clinical variables, we extracted data from the multimodality MRI clusters and ran correlation analyses with disease duration, VAS scores, HAMA, and HAMD scores.

3. Results

3.1. Demographic data and clinical characteristics of patients with classic trigeminal neuralgia and healthy controls

The demographic variables of the participants are summarized in **Table 1**. Sex and age did not differ between patients with CTN and healthy controls (sex: $P = 1.00$; age: $P = 0.989$). Compared with control subjects, patients had significantly higher scores on the HAMA [$t(36) = 6.58$, $P < 0.001$] and HAMD [$t(36) = 6.90$, $P < 0.001$]. The remaining characteristics did not differ significantly between groups.

3.2. Global tissue volume changes between patients with classic trigeminal neuralgia and healthy controls

Compared with healthy controls, patients with CTN exhibited slightly lower total GMV ($P = 0.042$; **Table 1**). There were no significant

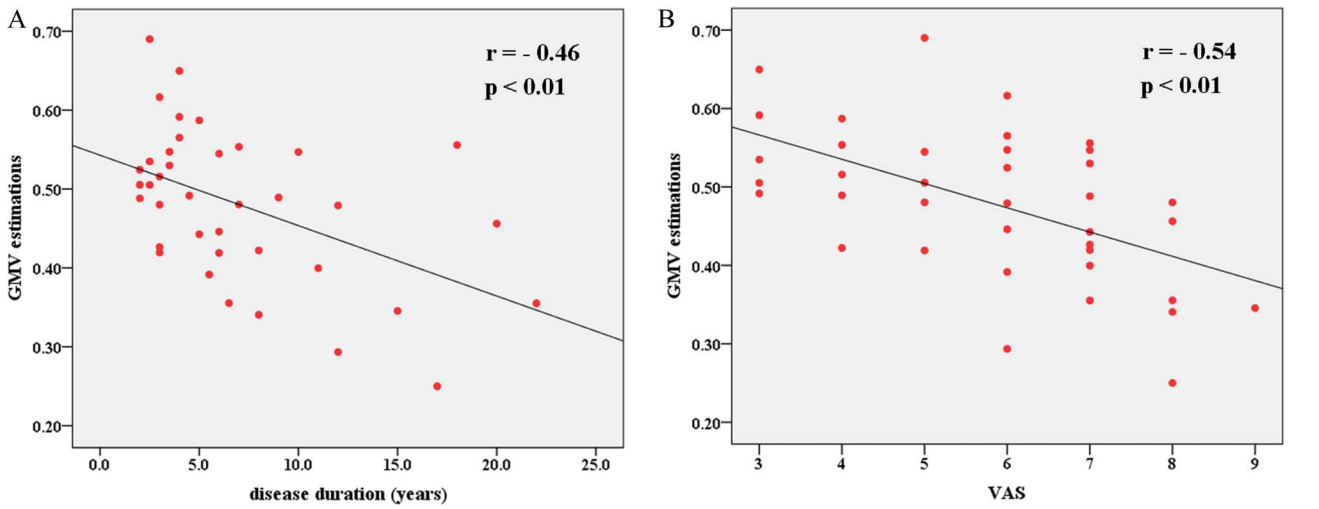

Figure 2. Negative correlations of GMV in the left inferior temporal gyrus with disease duration (A) and VAS (B) in patients with classic trigeminal neuralgia. GMV, gray matter volume; VAS, visual analogue scale.

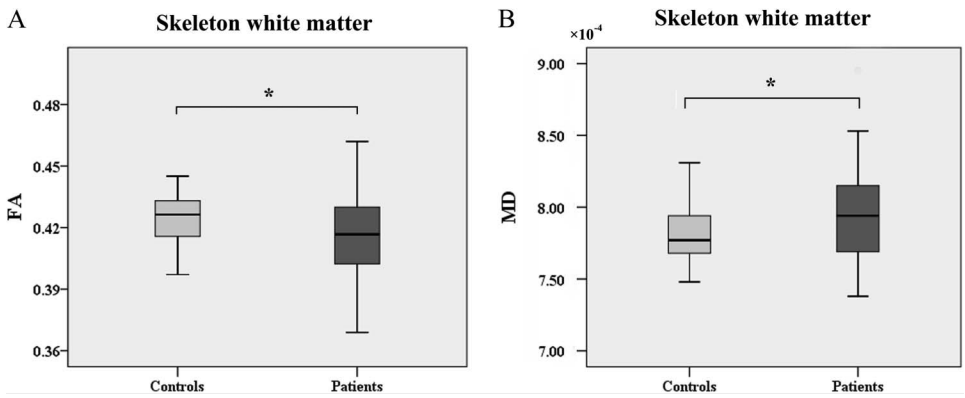

Figure 3. Group differences of mean fractional anisotropy (FA) and mean diffusivity (MD) in the skeletonized white matter between patients with classic trigeminal neuralgia and controls. Patients had lower skeleton FA (A) with higher skeleton MD (B). Asterisks (*) indicate $P < 0.05$.

differences in total intracranial volume ($P = 0.074$), white matter volume ($P = 0.238$), or CSF volume ($P = 0.276$) between the 2 groups. The 3D, T1 structural images of all participants showed no morphological abnormalities or apparent image artifacts.

3.3. Regional gray matter volume changes between patients with classic trigeminal neuralgia and healthy controls

Patients with CTN had widespread decreased GMV across the cerebral areas, including ACC, mid-cingulate cortex (MCC), insula, S2, primary motor cortex (M1), premotor area (PMA), and several portions of temporal lobe compared with that in controls, and increased GMV in a small part of the superior parietal lobule (SPL) ($P = 0.05$, FDR corrected at cluster level, **Fig. 1**; see **Table 2** for more details on the clusters, including MNI coordinates and Brodmann areas). Furthermore, there was a negative correlation of GMV in the left inferior temporal gyrus (ITG) with disease duration ($r = -0.46$; $P < 0.01$) and pain intensity ($r = -0.54$; $P < 0.01$) of the patients (**Fig. 2**). Anxiety and depression scores did not correlate with GMV in any of these brain regions in either group.

3.4. Tract-Based Spatial Statistics analysis

To investigate global differences in white matter integrity, we tested for group differences in FA and MD within the white matter skeleton. Compared with controls, patients with CTN showed 2.0% reduction in FA in skeletonized white matter (controls = 0.424 ± 0.013; patients = 0.416 ± 0.021; $P = 0.039$) (**Fig. 3A**). We also detected 1.7% higher MD within the white matter skeleton in patients with CTN

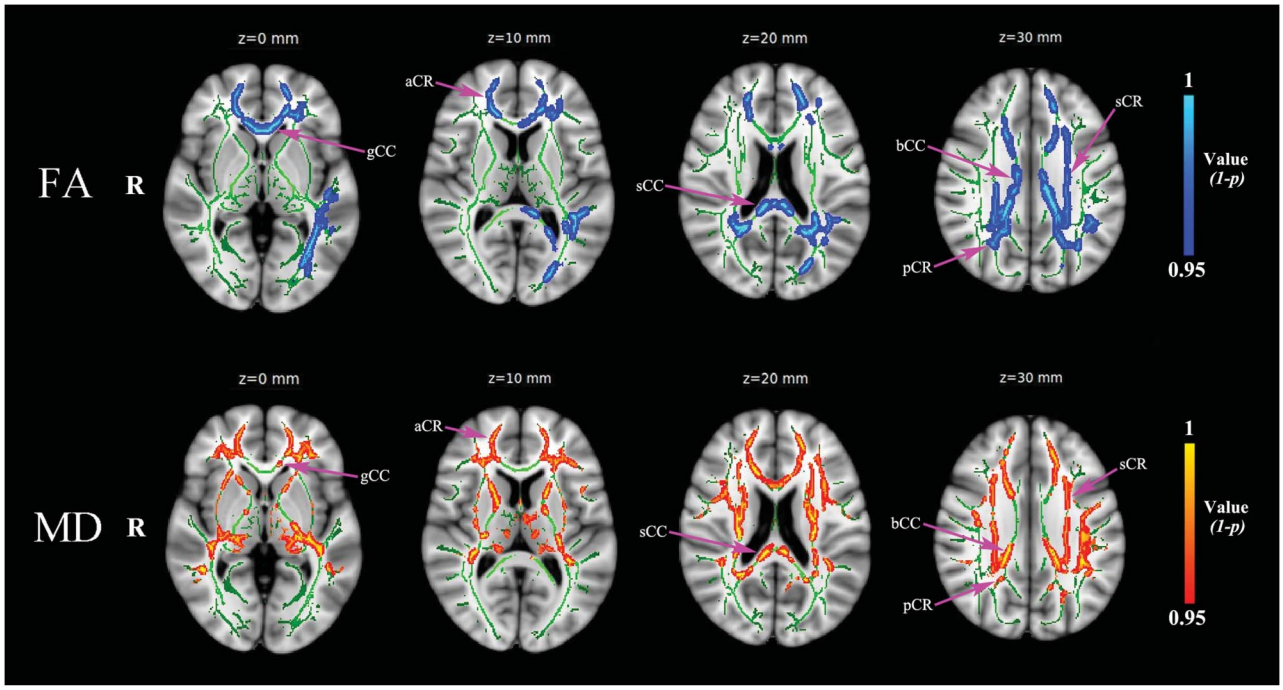

Figure 4. Fractional anisotropy (FA) and mean diffusivity (MD) differences in white matter between patients with classic trigeminal neuralgia and healthy controls ($P = 0.05$, FWE correction using threshold-free cluster enhancement). Blue clusters in the upper row indicate patients < controls (FA) and red clusters in the lower row meant patients > controls (MD). aCR, anterior corona radiata; bCC, body of cingulate cortex; gCC, genu of cingulate cortex; pCR, posterior corona radiata; sCC, splenium of cingulate cortex; sCR, superior corona radiata.

compared with control subjects (controls = [0.781 ± 0.018] × 10^{-3} mm^2/s; patients = [0.795 ± 0.032] × 10^{-3} mm^2/s; $P = 0.022$) (**Fig. 3B**).

Classic trigeminal neuralgia, compared with controls, had extensive reductions in FA and increases in MD in white matter across the brain ($P = 0.05$, FWE correction using TFCE; **Fig. 4** and **Table 3**). Specifically, FA was robustly lower (by 18%-30%) throughout the corpus callosum (genu, body, and splenium) in patients compared with controls, whereas MD was only 12% to 15% higher. Furthermore, patterns of lower FA and higher MD were also detected in the anterior, posterior, and superior corona radiata in the CTN group. Increased MD in patients was found in the bilateral inferior and superior cerebellar peduncle, the corticospinal tract, the thalamus, the anterior and posterior limb of internal capsule, the external capsule, and the superior longitudinal fasciculus ($P = 0.05$, FWE correction using TFCE; **Fig. 5**). There was no statistical difference in FA in these areas between groups.

3.5. Functional connectivity analysis

Using all of the clusters of the group differences in **Table 2**, we further investigated the ACC, MCC, insular cortex/S2, ITG, superior temporal gyrus , the left M1/PMA, and the right superior parietal lobule as our seed regions. The seed-to-voxel analysis revealed differences between the 2 groups only with the right insula/S2 as the seed (**Fig. 6**). Patients with CTN showed enhanced functional connectivity between the right insula/S2 and ACC, medial prefrontal cortex (mPFC), posterior cingulate cortex (PCC), and bilateral DLPFC (**Fig. 6** and **Table 4**). There were no areas of decreased functional connectivity between patients with CTN and control subjects with the right insula/S2 as the seed region. In addition, the connectivity strength of right insula/S2 to ACC in patients with CTN was negatively associated with pain intensity ($r = -0.575$, $P < 0.01$), anxiety ($r = -0.453$, $P < 0.05$), and depression indices ($r = -0.501$, $P < 0.01$) (**Fig. 7**).

Table 3

Group differences of FA and MD in the main regions of brain white matter.

	Patients with CTN		Control subjects	
	FA ($\bar{x}$ ± SD)	MD ($\bar{x}$ ± SD)*	FA ($\bar{x}$ ± SD)	MD ($\bar{x}$ ± SD)*
gCC	0.36 ± 0.10†	1.02 ± 0.30‡	0.50 ± 0.20	0.89 ± 0.21
bCC	0.30 ± 0.05†	1.15 ± 0.27†	0.36 ± 0.08	1.02 ± 0.15
sCC	0.35 ± 0.08†	1.18 ± 0.25†	0.49 ± 0.11	1.00 ± 0.20
aIC (left)	0.38 ± 0.09	1.02 ± 0.27†	0.39 ± 0.10	0.84 ± 0.08
aIC (right)	0.36 ± 0.08	0.95 ± 0.20†	0.38 ± 0.09	0.83 ± 0.14
pIC (left)	0.41 ± 0.14	0.98 ± 0.27†	0.43 ± 0.15	0.82 ± 0.18
pIC (right)	0.40 ± 0.12	1.02 ± 0.30†	0.41 ± 0.12	0.84 ± 0.25
EC (left)	0.34 ± 0.09	1.11 ± 0.30†	0.35 ± 0.10	0.86 ± 0.13
EC (right)	0.35 ± 0.10	1.16 ± 0.30†	0.37 ± 0.12	0.85 ± 0.13
aCR (left)	0.24 ± 0.09†	0.87 ± 0.24‡	0.38 ± 0.12	0.79 ± 0.13
aCR (right)	0.27 ± 0.10†	0.89 ± 0.24†	0.39 ± 0.12	0.78 ± 0.16
pCR (left)	0.32 ± 0.06‡	0.85 ± 0.19‡	0.36 ± 0.06	0.76 ± 0.09
pCR (right)	0.32 ± 0.05‡	0.86 ± 0.18‡	0.36 ± 0.06	0.77 ± 0.08
sCR (left)	0.29 ± 0.06†	0.91 ± 0.25‡	0.38 ± 0.07	0.81 ± 0.07
sCR (right)	0.28 ± 0.08†	0.91 ± 0.19†	0.38 ± 0.08	0.80 ± 0.06
SLF (left)	0.39 ± 0.10	0.92 ± 0.09†	0.41 ± 0.13	0.81 ± 0.07
SLF (right)	0.41 ± 0.12	0.90 ± 0.08†	0.42 ± 0.14	0.80 ± 0.06
CST (left)	0.30 ± 0.06	1.10 ± 0.26‡	0.32 ± 0.07	0.98 ± 0.20
SCP (left)	0.26 ± 0.05	1.44 ± 0.40†	0.28 ± 0.06	0.93 ± 0.25
ICP (left)	0.24 ± 0.04	1.47 ± 0.42†	0.25 ± 0.05	0.98 ± 0.27
ICP (right)	0.25 ± 0.04	1.52 ± 0.45†	0.27 ± 0.06	1.01 ± 0.28

P values are calculated based on independent-samples *t* test between 2 groups, as appropriate.
Diffusion in square millimeter/second.
$\bar{x}$, mean value; aCR, anterior corona radiata; aIC, anterior limb of internal capsule; bCC, body of corpus callosum; CTN, classic trigeminal neuralgia; CST, corticospinal tract; EC, external capsule; FA, fractional anisotropy; gCC, genu of corpus callosum; ICP, inferior cerebellar peduncle; MD, mean diffusivity; pCR, posterior corona radiata; pIC, posterior limb of internal capsule; sCC, splenium of corpus callosum; SCP, superior cerebellar peduncle; sCR, superior corona radiata; SLF, superior longitudinal fasciculus.
* For MD, values are $\times 10^{-3}$.
† $P < 0.01$.
‡ $P < 0.05$.

4. Discussions

This study investigated brain reorganization associated with CTN and its relationship to the duration and severity of orofacial pain, anxiety, and depression. Compared with healthy controls, patients with CTN had widespread structural brain alterations and increased functional connectivity of the right insula/S2. Furthermore, several changes were related to clinical variables. To date, there have been only 2 other fMRI studies on CTN[7,35] and none on resting-state functional connectivity. To our knowledge, this is the first study to combine structural MRI and rsfMRI to show brain pathophysiology in patients with CTN.

4.1. Morphological alterations in classic trigeminal neuralgia

4.1.1. Gray matter volume abnormalities

Extensive GMV reduction was demonstrated in bilateral temporal lobe in patients with CTN. The temporal lobe is involved in the processing of auditory perception, speech, language comprehension, and emotion.[45] Relatively few morphometric MRI studies have reported temporal lobe atrophy in chronic pain conditions, and findings were inconsistent.[5,21,50] Decreased GMV of the temporal lobe seems more common in CTN than other pain syndromes[26,37] and the reason still remains unknown. Furthermore, we found negative correlations between left ITG GMV and both duration and orofacial pain severity, which is consistent with previous research.[37] The ITG has largely been ignored in pain imaging studies, partly because many investigators restrict analyses and interpretation to regions more consistent with the "pain matrix," whereas the link between ITG and pain is unclear. A possible role of ITG is in mnemonic processes related to the affective component of pain, which may be linked to impaired memory in migraine patients.[51] Early research indicated the projections of ITG to the amygdala and hippocampus,[57] which are involved in emotional processing.[38] Our findings suggest that decreased GMV in the left ITG could be relevant to pain memory and affect in CTN and worsen with disease severity.

We also detected reduced GMV in the MCC of patients with CTN. Atrophic MCC has been reported in several chronic pain conditions, including low back pain,[20] temporomandibular disorder,[33] and fibromyalgia.[39] MCC is associated with pain-related fear-avoidance, environmental monitoring, and skeletomotor orientation.[52] This region is also involved in multidimensional modulation of nociceptive information, including pain sensation, negative affect, and cognitive control.[43] Thus, MCC could be related to both emotional and cognitive deficits of CTN.

Additionally, CTN group had decreased GMV of left M1 and PMA. Although the role of motor regions in pain is not fully

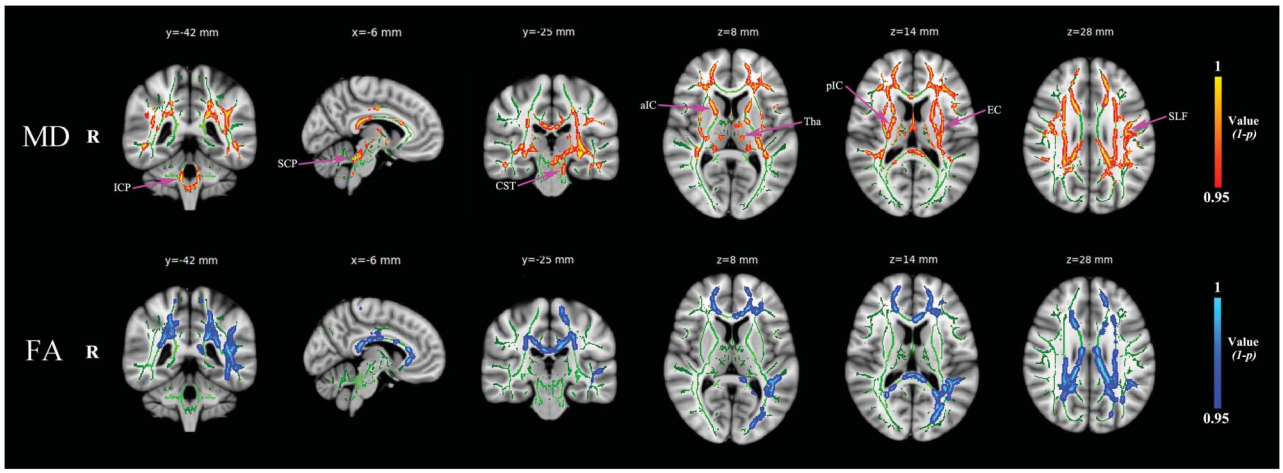

Figure 5. Regions of increased mean diffusivity (MD) (upper row) without distinction of fractional anisotropy (FA) (lower row) in classic trigeminal neuralgia compared with control group. aIC, anterior limb of internal capsule; CST, corticospinal tract; EC, external capsule; ICP, inferior cerebellar peduncle; pIC, posterior limb of internal capsule; SCP, superior cerebellar peduncle; SLF, superior longitudinal fasciculus; Tha, thalamus.

established, there is evidence suggesting that M1 is associated with pain modulation.[42] Motor abnormalities are supported by nocifensive behavior seen in temporomandibular disorder.[32,33] Furthermore, decreased GMV in motor areas could be related to an adaptive response to persistent nociceptive input or to an inhibition of jaw movement to avoid eliciting pain.[48]

4.1.2. White matter abnormalities

Patients with CTN had widespread reduced FA and increased MD, suggesting the disruption of integrity in global white matter and nociceptive tracts. It is well known that abnormal MD and FA existed in the root of trigeminal nerves in patients with CTN,[25,29] whereas only one recent study focused on white matter plasticity across the brain.[13] However, our result was a little different from this report. We found that patients had higher MD (without FA alterations) in the brainstem, thalamic radiation, internal capsule, and superior longitudinal fasciculus adjacent to sensorimotor cortex. Because these regions belong to the ascending nociceptive pathway, the average molecular motion of the pain-sensitive afferents is probably abnormal in the CTN group, which is inconsistent with that study reporting no changes in either MD or FA in these brain regions,[13] and the mechanisms are needed for further investigations.

Fractional anisotropy and MD abnormalities were fairly extensive across the corpus callosum and corona radiata in patients with CTN, suggesting possible deficits on the inter- and intra-hemispheric transmission of information. The frontoparietal cortices, which are connected by corpus callosum from corona radiata, are believed to participate in multisensory integration, such as the cognitive control, attention, and environmental reaction.[9,10] Meanwhile, decreased FA in corpus callosum have been reported in patients with lesions of the trigeminal lemniscus,[13,34] supporting the involvement of this region in CTN. Additionally, several white matter areas had connections with pain-related regions, including anterior corona radiata projecting to ACC[54] and external capsule adjacent to insula.[8] Reduced white matter integrity is also suggested by our findings of abnormal DTI metrics in the posterior and superior corona radiata (close to the posterior parietal cortex), which may be related to attention and reaction to the noxious threat in the surrounding environment.[3,27]

4.2. Alterations of functional connectivity

To our knowledge, this is the first report on abnormalities of resting-state functional connectivity in patients with CTN. We used brain regions with GMV reduction in patients with CTN as seeds to explore differences in connectivity between groups.

In contrast to healthy controls, patients with CTN had increased functional connectivity between the right insula/S2 seed and ACC, mPFC, PCC, and bilateral DLPFC. These findings mainly concern regions of 2 distinct networks: the salience network and the DMN. As the key nodes of salience

Table 4

Seed-based rsfMRI demonstrating significant difference in functional connectivity between CTN and control group.

Seed regions	Target regions	BA	Side	Voxels in cluster	MNI coordinate			Peak voxel *t* value
					x	y	z	
Insula/S2	ACC	32	Left	162	−6	50	9	3.5836
	mPFC	10	Right	128	12	45	21	4.2125
	PCC	31	Left	165	−6	−60	12	3.9655
	DLPFC	8	Left	225	−24	27	51	5.2488
	DLPFC	8	Right	139	20	30	54	3.5684

Data are thresholded of $P = 0.05$ with FDR correction at the cluster level for multiple comparisons.

ACC, anterior cingulate cortex; BA, Brodmann area; CTN, classic trigeminal neuralgia; DLPFC, dorsal lateral prefrontal cortex; mPFC, medial prefrontal cortex; PCC, posterior cingulate cortex; rsfMRI, resting-state functional magnetic resonance imaging; S2, secondary somatosensory cortex.

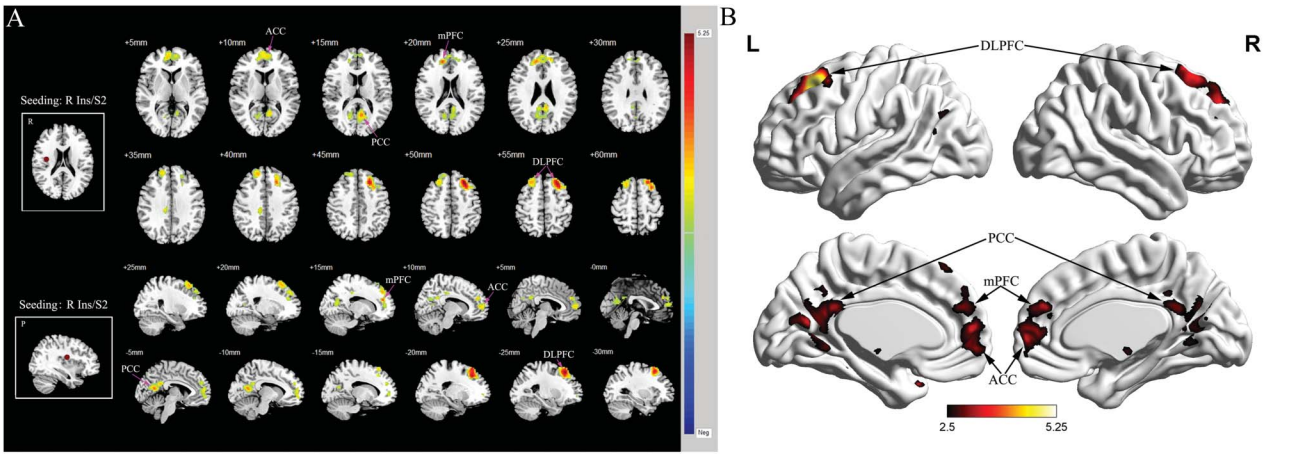

Figure 6. Enhanced functional connectivity of patients with classic trigeminal neuralgia in contrast to controls between the right insula/S2 seed and ACC, mPFC, PCC, and bilateral DLPFC. The right insula/S2 was chosen as the seeding area with 6 mm radius sphere for the analysis. (A) Axial and sagittal views; (B) Lateral and medial views of bilateral hemispheres. All images were shown with FDR correction at a cluster level of $P = 0.05$ for multiple comparisons. The color bar displayed *t*-values. ACC, anterior cingulate cortex; DLPFC, dorsolateral prefrontal cortex; mPFC, medial prefrontal cortex; PCC, posterior cingulate cortex; S2, secondary somatosensory cortex.

network, which overlaps considerably with the "pain matrix," ACC and the seed insula are sensitive to salient event, and one of their roles is to mark such event for special processing and initiate appropriate control for response.[31] Meanwhile, strong functional interaction between insula and ACC facilitates rapid access to the motor system.[31] Numerous nociceptive studies revealed coactivation of ACC and anterior insula in acute[16,53] and chronic pain.[41] Other evidence explores reciprocal connection of ACC to all major divisions of the insula.[43] In summary, the structural and functional alterations of anterior insula and ACC underlie the deficits of salient network in chronic pain conditions including CTN.

Meanwhile, less functional connectivity of the right insula to the ACC in CTN group was associated with higher clinical pain as well as greater anxiety and depression scores in the current study. The hyper-connection between anterior insula and ACC, which showed negative correlation with clinical pain ratings, was also displayed in the patients with temporomandibular disorder.[19] Anterior insula and ACC probably have a unique role in affective pain process.[60] Meanwhile, CTN might increase the risk of subsequent newly diagnosed depression, anxiety, and sleep disorder.[58] Based on the present and previous research, we conclude that the right insula–ACC connection may be vulnerable to the chronic pain disorder, suggesting that this functional alteration might serve as a preferable indicator for evaluation of both nociceptive and affective components in CTN.

We also notice that patients demonstrated enhanced functional connectivity of PCC and mPFC to the seed anterior insula, suggesting that these regions have dysfunctional pain processing across the CTN group. As crucial brain regions of DMN, PCC and mPFC show reliable deactivation during externally guided attention, especially on the focus of painful stimuli.[24] Given that most patients with CTN report sporadic but lancinating pain, perhaps anticipation of pain attack keeps their brains from being truly resting. So it is reasonable to expect that these patients have an altered brain resting state. Acute pain is known to induce deactivation on DMN,[24,40] and increased functional connectivity was also reported between DMN and anterior insula in patients with different persistent pain disorders.[4,23,36] Taken together, our findings add the knowledge that the abnormal insula–DMN connection could be an effect not only by continuous ongoing pain but also by intermittent pain condition.

Although bilateral DLPFC had increased connectivity to the right insula seed in patients with CTN, the connection was particularly strong for the left DLPFC. Dorsolateral prefrontal cortex has been proposed a central role in top–down pain processing,[28] and it has extensive connections with sensory and motor cortices and is useful for regulating attention, thought, and action.[2] Previous study concluded that left DLPFC displayed

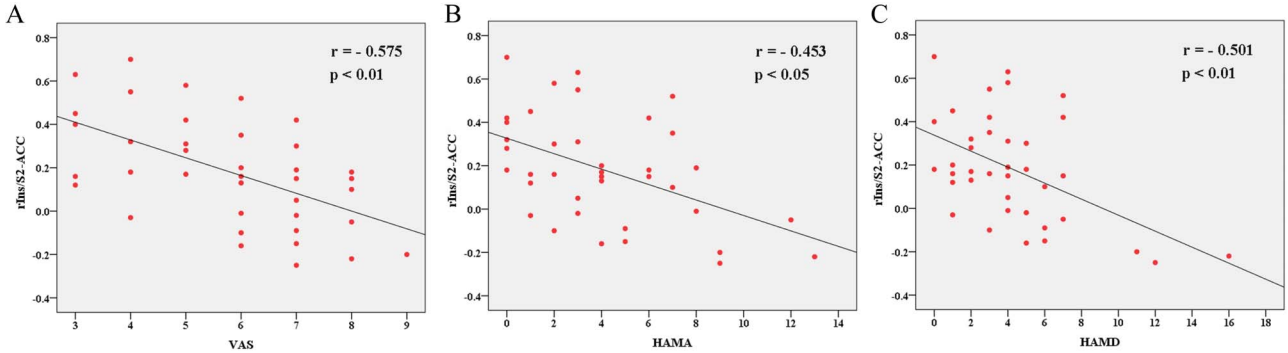

Figure 7. Functional connectivity of the right insular cortex/S2 to the ACC was negatively correlated with the scores of VAS (A), HAMA (B), and HAMD (C) in patients with CTN. ACC, anterior cingulate cortex; HAMA, Hamilton Anxiety Rating; HAMD, Hamilton Depression Rating; rIns, right insular cortex; S2, secondary somatosensory cortex; VAS, visual analogue scale.

negative association with pain affect, whereas right DLPFC primarily had reduced correlation with both pain intensity and unpleasantness.[28] However, left DLPFC activation was exhibited during cognitive task in chronic low back pain as well.[41] Thus, increased connectivity of the left DLPFC to the right insula in CTN could involve both cognitive and affective dimensions of pain.

4.3. Conclusion

We show distinct gray matter, white matter, and functional connectivity changes in patients with CTN compared with controls. Reduced GMV was extensive across the whole brain including ACC, MCC, insula/S2, and several temporal regions in CTN group, and increased MD without FA alterations were seen in the brainstem–thalamo–cortical projections in DTI analysis. Enhanced functional connectivity was observed between the right insula/S2 and ACC, mPFC, PCC, and bilateral DLPFC in CTN. Moreover, based on correlations between clinical variables and altered brain structure and function, we propose that GMV reduction of the left ITG might index orofacial pain severity and disease duration, whereas right insula–ACC connectivity could index pain severity and affective dysfunction. These findings help us better understand the pathophysiology of orofacial pain and provide insight to facilitate the development of new therapies for CTN.

Conflict of interest statement

The authors have no conflict of interest to declare.

Acknowledgments

The authors thank Dr Massieh Moayedi for assistance with DTI analysis; and Dr Shana Burrowes and Dr Jing Zhang for English language editing. This work was supported by the National Natural Science Foundation of China (No. 81301207), the Clinical Research Award of the First Affiliated Hospital of Xi'an Jiaotong University, China (No. XJTU1AF-CRF-2015-028) and Opening Project of Key Laboratory of Shaanxi Province for Craniofacial Precision Medicine Research, College of Stomatology, Xi'an Jiaotong University (No. 2016LHM-KFKT001).
Author contributions: Guarantor of integrity of the entire study: Y. Wang and M. Zhang. Study design: Y. Wang, D.-y. Cao, and M. Zhang. Definition of intellectual content: Y. Wang. Literature search: Y. Wang, B. Remeniuk, S. Krimmel, and D. A. Seminowicz. Data acquisition: Y. Wang and M. Zhang. Data analysis: Y. Wang, B. Remeniuk, S. Krimmel, and D. A. Seminowicz. Statistical analysis: Y. Wang and D. A. Seminowicz. Manuscript preparation: Y. Wang, D.-y. Cao, and M. Zhang. Manuscript editing: Y. Wang, B. Remeniuk, S. Krimmel, and D. A. Seminowicz. Manuscript review: D. A. Seminowicz and M. Zhang. M. Zhang and D.A. Seminowicz are joint corresponding authors.

Article history:
Received 7 December 2016
Received in revised form 5 May 2017
Accepted 10 May 2017
Available online 16 May 2017

References

[1] Antonini G, Di Pasquale A, Cruccu G, Truini A, Morino S, Saltelli G, Romano A, Trasimeni G, Vanacore N, Bozzao A. Magnetic resonance imaging contribution for diagnosing symptomatic neurovascular contact in classical trigeminal neuralgia: a blinded case-control study and meta-analysis. PAIN 2014;155:1464–71.
[2] Arnsten AF. Stress signalling pathways that impair prefrontal cortex structure and function. Nat Rev Neurosci 2009;10:410–22.
[3] Avillac M, Hamed SB, Duhamel JR. Multisensory integration in the ventral intraparietal area of the macaque monkey. J Neurosci 2007;27:1922–32.
[4] Baliki MN, Geha PY, Apkarian AV, Chialvo DR. Beyond feeling: chronic pain hurts the brain, disrupting the default-mode network dynamics. J Neurosci 2008;28:1398–403.
[5] Baliki MN, Schnitzer TJ, Bauer WR, Apkarian AV. Brain morphological signatures for chronic pain. PLoS One 2011;6:e26010.
[6] Bennetto L, Patel NK, Fuller G. Trigeminal neuralgia and its management. Br Med J 2007;7586:201.
[7] Blatow M, Nennig E, Sarpaczki E, Reinhardt J, Schlieter M, Herweh C, Rasche D, Tronnier VM, Sartor K, Stippich C. Altered somatosensory processing in trigeminal neuralgia. Hum Brain Mapp 2009;30:3495–508.
[8] Bushnell MC, Čeko M, Low LA. Cognitive and emotional control of pain and its disruption in chronic pain. Nat Rev Neurosci 2013;14:502–11.
[9] Cole MW, Repovš G, Anticevic A. The frontoparietal control system a central role in mental health. Neuroscientist 2014;20:652–64.
[10] Corbetta M, Kincade JM, Ollinger JM, McAvoy MP, Shulman GL. Voluntary orienting is dissociated from target detection in human posterior parietal cortex. Nat Neurosci 2000;3:292–7.
[11] Davis KD, Moayedi M. Central mechanisms of pain revealed through functional and structural MRI. J Neuroimmune Pharmacol 2013;8:518–34.
[12] DeSouza DD, Davis KD, Hodaie M. Reversal of insular and microstructural nerve abnormalities following effective surgical treatment for trigeminal neuralgia. PAIN 2015;156:1112–23.
[13] DeSouza DD, Hodaie M, Davis KD. Abnormal trigeminal nerve microstructure and brain white matter in idiopathic trigeminal neuralgia. PAIN 2014;155:37–44.
[14] Devor M, Govrin-Lippmann R, Rappaport ZH. Mechanism of trigeminal neuralgia: an ultrastructural analysis of trigeminal root specimens obtained during microvascular decompression surgery. J Neurosurg 2002;96:532–43.
[15] Dubner R, Sharav Y, Gracely RH, Price DD. Idiopathic trigeminal neuralgia: sensory features and pain mechanisms. PAIN 1987;31:23–33.
[16] Duerden EG, Albanese MC. Localization of pain-related brain activation: a meta-analysis of neuroimaging data. Hum Brain Mapp 2013;34:109–49.
[17] Fromm GH, Terrence CF, Maroon JC. Trigeminal neuralgia. Current concepts regarding etiology and pathogenesis. Arch Neurol 1984;41:1204–7.
[18] Hubbard CS, Khan SA, Keaser ML, Mathur VA, Goyal M, Seminowicz DA. Altered brain structure and function correlate with disease severity and pain catastrophizing in migraine patients. eNeuro 2014;1:e20.14.
[19] Ichesco E, Quintero A, Clauw DJ, Peltier S, Sundgren PM, Gerstner GE, Schmidt-Wilcke T. Altered functional connectivity between the insula and the cingulate cortex in patients with temporomandibular disorder: a pilot study. Headache 2012;52:441–54.
[20] Ivo R, Nicklas A, Dargel J, Sobottke R, Delank KS, Eysel P, Weber B. Brain structural and psychometric alterations in chronic low back pain. Eur Spine J 2013;22:1958–64.
[21] Jensen KB, Srinivasan P, Spaeth R, Tan Y, Kosek E, Petzke F, Carville S, Fransson P, Marcus H, Williams SC. Overlapping structural and functional brain changes in patients with long-term exposure to fibromyalgia pain. Arthritis Rheum 2013;65:3293–303.
[22] Kakizawa Y, Seguchi T, Kodama K, Ogiwara T, Sasaki T, Goto T, Hongo K. Anatomical study of the trigeminal and facial cranial nerves with the aid of 3.0-tesla magnetic resonance imaging. J Neurosurg 2008;108:483–90.
[23] Khan SA, Keaser ML, Meiller TF, Seminowicz DA. Altered structure and function in the hippocampus and medial prefrontal cortex in patients with burning mouth syndrome. PAIN 2014;155:1472–80.
[24] Kong J, Loggia ML, Zyloney C, Tu P, LaViolette P, Gollub RL. Exploring the brain in pain: activations, deactivations and their relation. PAIN 2010;148:257–67.
[25] Leal PRL, Roch JA, Hermier M, Souza MAN, Cristino-Filho G, Sindou M. Structural abnormalities of the trigeminal root revealed by diffusion tensor imaging in patients with trigeminal neuralgia caused by neurovascular compression: a prospective, double-blind, controlled study. PAIN 2011;152:2357–64.
[26] Li M, Yan J, Li S, Wang T, Zhan W, Wen H, Ma X, Zhang Y, Tian J, Jiang G. Reduced volume of gray matter in patients with trigeminal neuralgia. Brain Imaging Behav 2017;11:486–492.
[27] Lloyd D, Roberts N. Role for human posterior parietal cortex in visual processing of aversive objects in peripersonal space. J Neurophysiol 2006;95:205–14.

[28] Lorenz J, Minoshima S, Casey K. Keeping pain out of mind: the role of the dorsolateral prefrontal cortex in pain modulation. Brain 2003;126:1079–91.
[29] Lutz J, Linn J, Mehrkens JH, Thon N, Stahl R, Seelos K, Brückmann H, Holtmannspötter M. Trigeminal neuralgia due to neurovascular compression: high-spatial-resolution diffusion-tensor imaging reveals microstructural neural changes. Radiology 2011;258:524–30.
[30] Maarbjerg S, Wolfram F, Gozalov A, Olesen J, Bendtsen L. Significance of neurovascular contact in classical trigeminal neuralgia. Brain 2015;138: 311–19.
[31] Menon V, Uddin LQ. Saliency, switching, attention and control: a network model of insula function. Brain Struct Funct 2010;214:655–67.
[32] Moayedi M, Weissman-Fogel I, Crawley AP, Goldberg MB, Freeman BV, Tenenbaum HC, Davis KD. Contribution of chronic pain and neuroticism to abnormal forebrain gray matter in patients with temporomandibular disorder. NeuroImage 2011;55:277–86.
[33] Moayedi M, Weissman-Fogel I, Salomons TV, Crawley AP, Goldberg MB, Freeman BV, Tenenbaum HC, Davis KD. Abnormal gray matter aging in chronic pain patients. Brain Res 2012;1456:82–93.
[34] Moayedi M, Weissman-Fogel I, Salomons TV, Crawley AP, Goldberg MB, Freeman BV, Tenenbaum HC, Davis KD. White matter brain and trigeminal nerve abnormalities in temporomandibular disorder. PAIN 2012;153:1467–77.
[35] Moissetl X, Villainl N, Ducreuxl D, Serriel A, Cuninl G, Valadel D, Calvinol B, Bouhassiral D. Functional brain imaging of trigeminal neuralgia. Eur J Pain 2011;15:124–31.
[36] Napadow V, LaCount L, Park K, As-Sanie S, Clauw DJ, Harris RE. Intrinsic brain connectivity in fibromyalgia is associated with chronic pain intensity. Arthritis Rheum 2010;62:2545–55.
[37] Obermann M, Rodriguez-Raecke R, Naegel S, Holle D, Mueller D, Yoon MS, Theysohn N, Blex S, Diener HC, Katsarava Z. Gray matter volume reduction reflects chronic pain in trigeminal neuralgia. NeuroImage 2013; 74:352–8.
[38] Price DD. Psychological and neural mechanisms of the affective dimension of pain. Science 2000;288:1769–72.
[39] Robinson ME, Craggs JG, Price DD, Perlstein WM, Staud R. Gray matter volumes of pain-related brain areas are decreased in fibromyalgia syndrome. J Pain 2011;12:436–43.
[40] Seminowicz DA, Davis KD. Pain enhances functional connectivity of a brain network evoked by performance of a cognitive task. J Neurophysiol 2007; 97:3651–9.
[41] Seminowicz DA, Wideman TH, Naso L, Hatami-Khoroushahi Z, Fallatah S, Ware MA, Jarzem P, Bushnell MC, Shir Y, Ouellet JA. Effective treatment of chronic low back pain in humans reverses abnormal brain anatomy and function. J Neurosci 2011;31:7540–50.
[42] Sessle B. Mechanisms of oral somatosensory and motor functions and their clinical correlates. J Oral Rehabil 2006;33:243–61.
[43] Shackman AJ, Salomons TV, Slagter HA, Fox AS, Winter JJ, Davidson RJ. The integration of negative affect, pain and cognitive control in the cingulate cortex. Nat Rev Neurosci 2011;12:154–67.
[44] Smith SM, Jenkinson M, Johansen-Berg H, Rueckert D, Nichols TE, Mackay CE, Watkins KE, Ciccarelli O, Cader MZ, Matthews PM. Tract-based spatial statistics: voxelwise analysis of multi-subject diffusion data. NeuroImage 2006;31:1487–505.
[45] Smith EE, Kosslyn SM, Smith E, Kosslyn S. Motor cognition and mental simulation. Cogn Psychol Mind Brain 2007:451–81.
[46] Society HCCotIH. The international classification of headache disorders, (beta version). Cephalalgia 2013;33:629–808.
[47] Song XW, Dong ZY, Long XY, Li SF, Zuo XN, Zhu CZ, He Y, Yan CG, Zang YF. REST: a toolkit for resting-state functional magnetic resonance imaging data processing. PLoS One 2011;6:e25031.
[48] Svensson P, Graven-Nielsen T. Craniofacial muscle pain: review of mechanisms and clinical manifestations. J Orofacial Pain 2001;15:117.
[49] Tölle T, Dukes E, Sadosky A. Patient burden of trigeminal neuralgia: results from a cross-sectional survey of health state impairment and treatment patterns in six European countries. Pain Pract 2006;6: 153–60.
[50] Tu CH, Niddam DM, Chao HT, Chen LF, Chen YS, Wu YT, Yeh TC, Lirng JF, Hsieh JC. Brain morphological changes associated with cyclic menstrual pain. PAIN 2010;150:462–8.
[51] Vincent M, Hadjikhani N. Migraine aura and related phenomena: beyond scotomata and scintillations. Cephalalgia 2007;27:1368–77.
[52] Vogt BA. Pain and emotion interactions in subregions of the cingulate gyrus. Nat Rev Neurosci 2005;6:533–44.
[53] Wager TD, Atlas LY, Lindquist MA, Roy M, Woo CW, Kross E. An fMRI-based neurologic signature of physical pain. New Engl J Med 2013;368: 1388–97.
[54] Wakana S, Jiang H, Nagae-Poetscher LM, Van Zijl PC, Mori S. Fiber tract–based atlas of human white matter anatomy 1. Radiology 2004; 230:77–87.
[55] Wang Y, Li D, Bao F, Guo C, Ma S, Zhang M. Microstructural abnormalities of the trigeminal nerve correlate with pain severity and concomitant emotional dysfunctions in idiopathic trigeminal neuralgia: za randomized, prospective, double-blind study. Magn Reson Imaging 2016;34:609–16.
[56] Wang Y, Li D, Bao F, Ma S, Guo C, Jin C, Zhang M. Thalamic metabolic alterations with cognitive dysfunction in idiopathic trigeminal neuralgia: a multivoxel spectroscopy study. Neuroradiology 2014;56:685–93.
[57] Webster M, Ungerleider L, Bachevalier J. Connections of inferior temporal areas TE and TEO with medial temporal-lobe structures in infant and adult monkeys. J Neurosci 1991;11:1095–116.
[58] Wu TH, Hu LY, Lu T, Chen PM, Chen HJ, Shen CC, Wen CH. Risk of psychiatric disorders following trigeminal neuralgia: a nationwide population-based retrospective cohort study. J Headache Pain 2015; 16:64.
[59] Yan C, Zang Y. DPARSF: a MATLAB toolbox for "pipeline" data analysis of resting-state fMRI. Front Syst Neurosci 2010;4:13.
[60] Yuan W, Dan L, Netra R, Shaohui M, Chenwang J, Ming Z. A pharmaco-fMRI study on pain networks induced by electrical stimulation after sumatriptan injection. Exp Brain Res 2013;226:15–24.
[61] Yu D, Yuan K, Zhao L, Dong M, Liu P, Yang X, Liu J, Sun J, Zhou G, Xue T. White matter integrity affected by depressive symptoms in migraine without aura: a tract-based spatial statistics study. NMR Biomed 2013; 26:1103–12.
[62] Zakrzewska JM, Akram H. Neurosurgical interventions for the treatment of classical trigeminal neuralgia. Cochrane Database Syst Rev 2010: 81–2.